NANOSYSTEMS

PECULIARITIES OF CURRENT TRANSPORT IN TITANIUM OXIDE–SILICON HETEROSTRUCTURES

YU.S. MILOVANOV,[1] I.V. GAVRILCHENKO,[1] V.YA. GAYVORONSKY,[2] G.V. KUZNETSOV,[1] V.A. SKRYSHEVSKY[1]

[1]**Institute of High Technologies, Taras Shevchenko National University of Kyiv**
(64, Volodymyrska Str., Kyiv 01601, Ukraine; e-mail: juri_milovanov@yahoo.com)

[2]**Institute of Physics, Nat. Acad. of Sci. of Ukraine**
(46, Prosp. Nauky, Kyiv 03028, Ukraine)

The mechanisms of charge carrier injection into Ti–TiO$_2$–(n,p)-Si heterostructures have been studied. The influence of the porous TiO$_2$ structure and the silicon substrate type on the electrical characteristics of heterostructures is analyzed. The charge transfer is shown to be accompanied by the appearance of a compensating polarization charge on the surface of TiO$_2$ nanoparticles. Correlations between the type of adsorbed molecules and the conditions of the current flow have been determined. In Ti–TiO$_2$–p-Si heterostructures, a change of the ratio between the numbers of injected electrons and holes can lead to the negative-conductivity effect.

1. Introduction

Recently, the considerable attention has been paid to studying the nanocrystalline oxide materials, which possess unique properties and wide application capabilities. Those compounds include titanium oxide TiO$_2$, a chemically stable inexpensive substance, which is widely used in the fabrication of gas sensors [1–3], film coatings [4], and injection solar cells [5, 6]. Titanium dioxide has unique photocatalytic properties [7, 8], being a promising material in the manufacture of photonic crystals [9].

Modern solution-based technologies of production of nanocrystalline titanium oxide ensure the stability of its chemical composition, as well as the reproducibility and controllability of its microstructure (the size of crystallites, size and volume of pores, specific surface area). The widely spread methods of the sol-gel technology allow one to synthesize fine-dispersed oxide films with a wide distribution of nanocrystallite dimensions [10, 11].

The reduction of crystallite dimensions to a threshold value ($d < 10$ nm) is accompanied by both a drastic growth of the role played by the surface energy and the corresponding modification of physico-chemical properties. For porous titanium oxide, the processes of charge carrier transport were studied, and the relevant drift mobility and lifetimes of electrons and holes were determined [12–14]. The electron transport in a wide-band-gap oxide material is substantially affected by the processes of charge carrier injection and their capture, at tunneling, onto the energy levels in the energy gap [6, 15]. In nanostructured materials, the situation becomes even more complicated due to the presence of a significant amount of electron capture centers located on the developed internal surface, with the concentration of those centers attaining 10^{18} cm^{-3} [16]. In massive TiO$_2$ crystals, the majority of injected carriers disappear in the course of bulk recombination. At the same time, in nano-sized crystallites, the charge carriers have enough time to reach intercrystallite boundaries and to be captured by surface traps. The electron transport in porous oxide semiconductors is very sensitive to adsorbed molecules, which considerably change the charge state of the internal surface. In particular, the adsorption of polar molecules (of water or ethyl alcohol) favors the controllable formation of charge carrier capture centers on the surface [1], which govern the injection features of nanostructured material.

The peculiarities of the injection mechanisms of charge carrier transport in the contacts between nanostructured TiO$_2$ and other semiconductors–in particular, silicon–
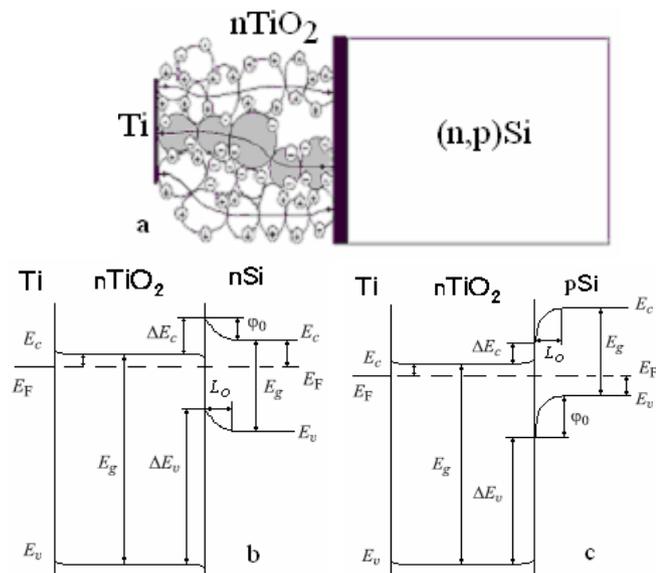
Fig. 1. Structure (*a*) and energy diagrams of Ti–TiO$_2$–*n*-Si (*b*) and Ti–TiO$_2$–*p*-Si (*c*) heterostructures

were practically not studied [1, 6]. Such heterostructures provide additional capabilities to control the injection fluxes of charge carriers and their capture by energy traps. In this work, we studied the mechanisms of charge carrier transport in structures with nanocrystalline TiO$_2$ films formed within methods of the sol-gel technology on single-crystalline silicon substrates with various types of conductivity: metal–TiO$_2$–*n*-Si and metal–TiO$_2$–*p*-Si. The electric properties of heterostructures were researched in various gaseous environments (air, water vapor, and ethyl alcohol vapor).

2. Experimental Technique

Titanium dioxide films were synthesized by the sol-gel method. Titanium tetraisopropoxide and α-terpineol were added to isopropanol, which was used as a solvent. α-terpineol provided an additional viscosity to the solution. To form porous films, polyethylene glycols with molecular masses $M = 300$ g/mol (specimens TiO$_2$-300) and $M = 1000$ g/mol (specimens TiO$_2$-1000) were used as complex-forming reagents. The TiO$_2$ concentration in the precursor was about 4 wt.%.

Oxide films were deposited onto the surface of a silicon wafer by pulling from the precursor and subjecting them to a subsequent annealing at a temperature of 450 °C. Such a treatment ensured a complete removal of organic compounds from the specimen and the formation of the

nanocrystalline anatase phase of TiO$_2$ [8]. According to the data of transmission electron microscopy, the average diameter of nanocrystallites in TiO$_2$-1000 specimens was 15 nm (a surface area of about 70 m^2/g), whereas two groups of nanocrystallites with average diameters of 3 and 20 nm were distinguished in TiO$_2$-300 specimens (a surface area of 100 m^2/g). The oxide layer porosity was calculated using the following formula, which takes the irregularities in the shape of particles into account [17]:

$$P\frac{1 - \varepsilon_{\rm eff}}{1 + 2\varepsilon_{\rm eff}} + (1 - P)\frac{\varepsilon_{\rm TiO_2} - \varepsilon_{\rm eff}}{\varepsilon_{\rm TiO_2} + 2\varepsilon_{\rm eff}} = 0\,, \qquad (1)$$

where P is the porosity, and $\varepsilon_{\rm eff}$ and $\varepsilon_{\rm TiO_2}$ are the dielectric permittivities of the porous medium and the solid-state anatase phase ($\varepsilon_{\rm TiO_2} = 40$), respectively. The porosity was 33–35% for TiO$_2$-1000 specimens and 38–40% for TiO$_2$-300 ones.

For the electric measurements, a Ti contact 30 nm in thickness and 1 mm in diameter was deposited onto the layer of porous titanium oxide with the use of the electron-beam evaporation technique. The diffusion of the donor titanium impurity resulted in a reduction of the contact resistance and stimulated the *p*-type conductivity in the TiO$_2$ oxide film. The electric parameters of fabricated heterostructures were studied by means of impedance spectroscopy and by measuring their current-voltage (I–V) and capacitance-voltage (C–V) characteristics [18].

Water or ethyl alcohol vapor was inlet into the chamber containing a specimen using a system of pumping through water or an aqueous solution of alcohol. Nitrogen vapor, which does not affect the electrophysical and optical properties of the examined structures, was used as a carrier gas.

3. Experimental Results and Their Discussion

3.1. I–V characteristics

The conductance of Ti–TiO$_2$–(n, p)-Si heterostructures is equal to the sum of conductances of the intermediate nanostructured oxide layer and the space charge barrier region in the semiconductor (Fig. 1). The structures have rectifying I–V characteristics, with the sign of rectification being in agreement with the type of silicon substrate conductivity.

Figure 1 illustrates the structure and the energy diagrams of Ti–TiO$_2$–(n, p)-Si heterostructures reproduced on the basis of known values for the energy gap widths $E_g({\rm TiO_2}) = 3.1$ eV and $E_g({\rm Si}) = 1.1$ eV, the electron affinity energies $\chi({\rm TiO_2}) = 4.3$ eV and $\chi({\rm Si}) = 4.0$ eV,
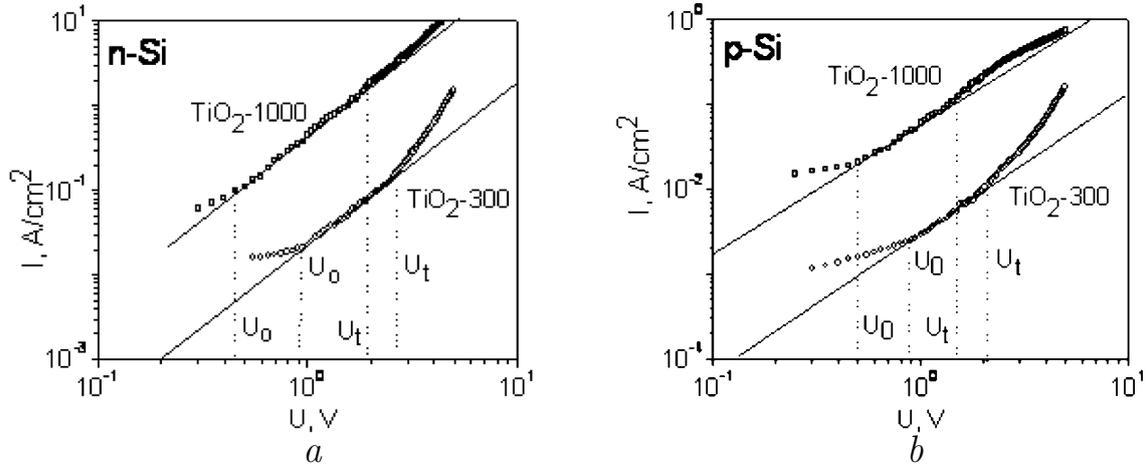
Fig. 2. I–V characteristics of Ti–TiO$_2$–n-Si (a) and Ti–TiO$_2$–p-Si (b) structures in SCLC coordinates

and the work function $\Psi(\text{Ti}) = 4.4$ eV [17, 19]. The Fermi level energy E_{F}, the potential barrier height φ_0, and the energy discontinuities in the conduction, ΔE_c, and valence, ΔE_v, bands were determined with regard for the experimentally measured values of charge carrier concentration in TiO$_2$ and Si. For isotype Ti–TiO$_2$–(n, p)-Si heterostructures, the parameters indicated in Fig. 1 have the following values: $E_c - E_{\text{F}} = 0.1$ eV (n-TiO$_2$), $E_c - E_{\text{F}} = 0.2$ eV (nSi), $\varphi_0 = 0.2$ eV, $\Delta E_c = 0.3$ eV, and $\Delta E_v = 2.3$ eV (the barrier for a current in the conduction band). The corresponding parameters for anisotype Ti–TiO$_2$–pSi heterostructures are $E_c - E_{\text{F}} = 0.1$ eV (n-TiO$_2$), $E_{\text{F}} - E_v = 0.2$ eV (p-Si), $\varphi_0 = 0.5$ eV, $\Delta E_c = 0.3$ eV, and $\Delta E_v = 2.3$ eV (the barrier for a current in the valence band). The estimations of the depletion region thickness L_o in TiO$_2$ and Si, according to work [17], brought about the relation $L_o(\text{Si}) \gg L_o(\text{TiO}_2)$; i.e. the space charge region in the examined heterostructures can be considered as completely located in silicon.

If the space charge region in silicon is connected directly, its resistance considerably decreases as the voltage grows, and the contribution of high-resistance oxide layer dominates. In Fig. 2, the dependences of the current on the external voltage are depicted for the direct connection of Ti–TiO$_2$–n-Si (a positive potential on the titanium contact) and Ti–TiO$_2$–p-Si (a negative potential on the titanium contact) structures. On the log-log scale, lg I versus lg U, the I–V characteristic has linear sections different by their slopes: the Ohm law is obeyed at the initial stage, a quadratic dependence $I \sim U^2$ is typical of the voltage interval $U \approx 1 \div 5$ V, and the further voltage increase is accompanied by an accelerated current growth. The square-law current dependence on

the voltage observed in the structures concerned is typical of space-charge-limited currents (SCLCs).

Within the initial Ohmic section of the I–V characteristic, the concentration of charge carriers is close to the equilibrium one, which allows the specific resistance of an oxide film to be determined. The specific resistance of oxide layers in more ordered and homogeneous TiO$_2$-1000 specimens was $\rho \approx 10^4 \div 10^5\ \Omega \cdot$ cm. In TiO$_2$-300 specimens, a more disordered structure and a larger area of the specific surface give rise to an increase in the concentration of surface capture centers and the corresponding growth of the specific resistance to $\rho \approx 10^6\ \Omega \cdot$ cm. In addition, the presence of two nanocrystallite groups with different dimensions in TiO$_2$-300 specimens intensifies the intercrystallite diffusion of charge carriers, which can also be captured by molecular traps [8].

The concentration of equilibrium free charge carriers n_0 and their drift mobility μ in the oxide layer were determined in different sections of the I–V characteristic following different formulas: in the ohmic interval, according to the expression [19]

$$I = e n_0 \mu \frac{U}{L};\qquad (2)$$

in the square-law region, according to the relation

$$I = \frac{\mu \varepsilon \varepsilon_0 U^2}{L^3};\qquad (3)$$

and on the basis of the voltage U_0 of transition from the linear dependence to the square-law one,

$$U_0 = \frac{4 e n_0 L^2}{3 \varepsilon \varepsilon_0},\qquad (4)$$

where U is the voltage across the structure, I the corresponding current density, μ the charge carrier mobility,

ε the dielectric constant of the oxide layer, ε_0 the dielectric permittivity of vacuum, n_0 the equilibrium concentration of charge carriers, and L the thickness of the TiO$_2$ layer. The coincidence of values obtained for the concentration, $n_0 \approx 1 \times 10^{17}$ cm^{-3}, and the mobility, $\mu \approx 10^{-3} \div 10^{-4}$ cm^{2}V^{-1}s^{-1}, using different methods confirms the validity of our assumption about the dominating contribution made by SCLCs.

The temperature dependence of the drift mobility in the temperature interval $T = 300 \div 400$ K is characterized by the activation energy $E_\mu \approx 0.13 \div 0.15$ eV. We may suppose that the charge carriers are transported through the TiO$_2$ layer by means of the mechanism of hopping over localized electron states. In the case of the hopping mechanism, the drift mobility is evaluated by the expression

$$\mu = \frac{e\nu R^2}{6kT} \exp\left(-\frac{E_\mu}{kT} - \frac{R}{r}\right), \tag{5}$$

where ν is the phonon frequency, R the hopping distance, and r the localization radius. At the characteristic values of phonon frequency $\nu \approx 10^{12}$ s^{-1}, the obtained mobility values $\mu \approx 10^{-3} \div 10^{-4}$ cm^{2}V^{-1}s^{-1} correspond to the hopping distance $R < 1$ nm, which is comparable with interatomic distances in the TiO$_2$ layer.

An important factor that affects the electric conductivity in nanostructured titanium oxide is the presence of a significant number of charge carrier capture centers [20]. In the SCLC case, the trap concentration N_t can be evaluated on the basis of the threshold voltage of their filling, U_t, by the formula (Fig. 2)

$$U_t = \frac{eN_t L^2}{2\varepsilon\varepsilon_o}. \tag{6}$$

For TiO$_2$-1000 specimens, the concentration of capture centers is $N_i \sim 10^{16}$ cm^{-3}, which is 3 to 5 times lower than that for TiO$_2$-300 ones. This estimate agrees with the results obtained for defect centers in nanocrystalline anatase using the electron paramagnetic resonance spectroscopy method [8].

The influence of the conductivity type in the silicon semiconductor substrate on the charge carrier transport can be estimated by analyzing the dependences of the conductance G of Ti–TiO$_2$–n-Si and Ti–TiO$_2$–p-Si structures on the external voltage U, which are depicted in Fig. 3. One can observe that the G versus U curve is asymmetric with respect to the voltage polarity. Such a behavior is governed by a rectifying potential barrier at the interface between the TiO$_2$ oxide layer and the silicon substrate.

In the case of Ti–TiO$_2$–n-Si structures, the regime of monopolar electron injection into the oxide layer is realized. Depending on the applied voltage polarity, either the Ti or n-Si electrode plays the role of injecting cathode. The violation of electroneutrality in the specimen bulk induces a confinement of the current by the arising space charge. All injected electrons remain to stay in the conduction band and take part in both the formation of space charge in the bulk and the charge transfer. If the voltage U in the direct direction exceeds 3–4 V, the current saturation is observed, which is associated with minor changes in the concentration of charge carriers injected into the TiO$_2$ layer. In this case, the square-law current dependence, which is characteristic of the SCLC, transforms to that occurring in the low-signal regime (Fig. 2,a).

In TiO$_2$–p-Si structures connected in the direct direction, the regime of charge carrier double injection of electrons from the titanium electrode and holes from the directly biased TiO$_2$–p-Si heterojunction into the TiO$_2$ oxide layer is realized. At the initial stage ($U < 0$), the recombination of injected minority charge carriers gives rise to a reduction of the electron concentration, which results in the appearance of an interval with a negative conductance (Fig. 3,b; curves 1 and 2). The effect of negative differential conductance associated with the presence of deep traps in TiO$_2$ with an activation energy of 175–375 meV has already been observed by us in TiO$_2$-based heterostructures [20].

If the applied voltage grows further ($U > 5$ V), the neutralizing flux of injected electrons becomes the basic current component in the high-injection region, which stimulates the process of conductance growth. If the level of bipolar injection is considerable, the electric neutrality is established within the transit time interval, so that the current becomes limited not only by the recombination, but also by the arising space charge of captured and free carriers. The increase of the electron-hole pair concentration and the corresponding growth of the oxide-layer conductance are more pronounced for homogeneous specimens of the TiO$_2$-1000 type (Fig. 1,b).

If the voltage polarity is opposite (a positive potential is applied to the Ti contact), the role of the electron and hole components in the injection current becomes insignificant in Ti–TiO$_2$–p-Si structures. A deviation from the profile typical of SCLC may be associated with the influence of an oppositely connected potential barrier at the interface between the oxide layer and the p-Si substrate.

The magnitude of negative conductance effect is affected substantially by the structure parameters and
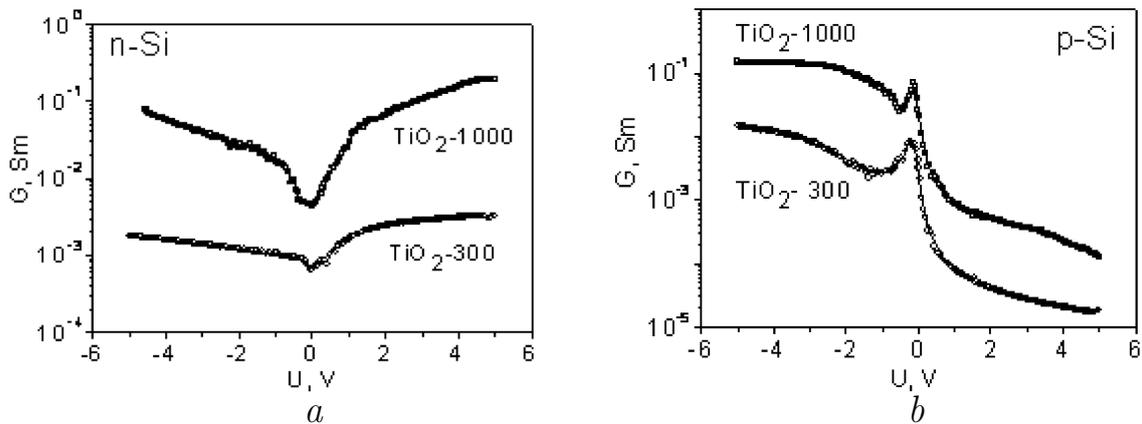
Fig. 3. Dependence of the conductance on the applied voltage for Ti–TiO$_2$–n-Si (a) and Ti–TiO$_2$–p-Si (b) structures

the measurement conditions (the frequency, temperature, composition of gas environment). In TiO$_2$-1000 specimens, the differential conductance at the frequency $f = 10^6$ Hz is by 2 to 3 orders of magnitude higher than that in TiO$_2$-300 specimens with the same thickness of the oxide layer, which is in agreement with the results of dc conductance measurements. At a temperature elevation, the capacitance and the conductance of heterostructures grow in the whole range of frequencies, which is connected with the increase in the concentration of thermally equilibrium electron–hole pairs and the modification of their charge ratios.

3.2. Formation of conduction channels

The processes of electron transport in a porous TiO$_2$ layer can be interpreted in the framework of the mechanism of charge carrier transport in such a disperse system as coupled TiO$_2$ nanocrystallites (Fig. 1,a). Some authors treat the conductance of a porous oxide layer from the viewpoint of charge carrier transit time [21]. In work [22], a scheme was proposed for the formation of conduction channels for injected charge carriers, which takes the role of the charge state of the internal surface in the oxide layer into account. The formation of charge carrier transport paths and the transit time depend on the injection conditions, the nature and the filling degree of traps located on the surface and in the bulk, and the local polarization charge of a nanocrystallite. The charge sign is determined by the types of preceding and adsorbed surface centers (it is positive for donors and negative for acceptors). The magnitude of surface charge depends not only on the concentration and the filling degree of surface traps, but also on the polarization of available dipole molecules.

In the examined structures, the dimensions of TiO$_2$ nanoparticles were comparable with the screening length, which resulted in the almost complete flattening of energy bands and a uniform charge distribution over the crystallite volume. The positive surface charge induced an elevation of the Fermi level and the accumulation of injected electrons in the crystallite bulk. The formation of conduction paths took place under the conditions, when the total electric field in the oxide layer was nonuniform, and some time was required for the saturation of traps and for the polarization of TiO$_2$ nanoparticles to complete. In the case of electron injection, electrons were captured firstly by traps in TiO$_2$ nanoparticles, which were located near the titanium cathode, and formed a screening polarization positive charge on their surface. Gradually, the electrons penetrated further in the oxide layer bulk and form conduction channels with the positively charged surface of nanoparticles (Fig. 1, nonshaded channel). The injection of holes is blocked in such a channel by an electric field that arises at the polarization. If the surface charge is negative, the channels, which are conducting for holes and, simultaneously, blocked for electrons, are formed in the system of nanocrystallites (Fig. 1, shaded channel).

3.3. Adsorption effect

Adsorption is one of the effective methods to vary the concentration and the charge state of surface traps. The magnitude of generated surface charge depends on the capability of adsorbate atoms to capture or donate an electron. It is known that oxygen-containing radical groups are intensively formed on the internal surface of nanocrystalline TiO$_2$ under environmental conditions. Those groups to a great extent govern the processes of
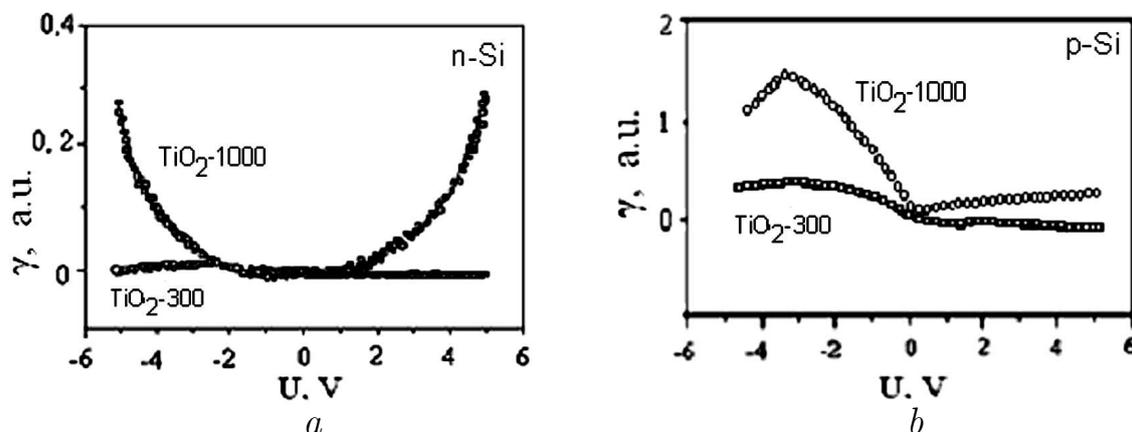
Fig. 4. Dependences of the adsorption sensitivity on the voltage for Ti–TiO$_2$–n-Si (a) and Ti–TiO$_2$–p-Si (b) structures at their blowing with H$_2$O vapor

acceptor-donor interaction with injected charge carriers [8].

Adsorbate atoms, when having got on the semiconductor surface, try to capture or donate an electron, depending on their physico-chemical properties. In the air environment, oxygen is intensively adsorbed onto the surface of nanocrystallites. Oxygen atoms, which are characterized by a high electronegativity, localize a semiconductor's electron in their vicinity to form acceptor anion-radicals O^{2-} and O^{3-}. Water vapor is another important gas component of the environment. Its molecules are characterized by a substantial dipole moment. H$_2$O molecules dissociate on the pore surface, the opposite charges being separated owing to the difference between their diffusion coefficients in the oxide film (H$^+$ ions are mobile, whereas OH$^-$ ones are localized at hydroxyl groups). Water dissociation is also promoted by the presence of chemisorbed oxygen on the oxide surface, which can also stimulate the growth of the oxide layer conductance following the reaction H$_2$O + O$^-$ + e^- → 2OH$^-$. Porous titanium oxide is a hydrophilic substance, which contains some adsorbed water, even if being in a dry atmosphere. Adsorbed donor water molecules donate electrons to the conduction band or a center on the semiconductor surface and form positively charged surface molecular groups (HO$_2$)$^+$ or (OH)$^-$.

The adsorption sensitivity was evaluated by the relative variation of the conductance, $\gamma = \frac{G_A - G_0}{G_0}$, where G_0 and G_A are the electric conductances of the specimen in air and when being purged with saturated water vapor, respectively (Fig. 4).

A positive charge at the internal surface of porous TiO$_2$ was provided by the adsorption of donor molecules from the gas environment containing water and ethanol vapors, the corresponding molecules being characterized by considerable dipole moments. Blowing the TiO$_2$ surface with water or alcohol vapor under the condition that the gradient of its partial pressure is constant activates donor-acceptor transport processes and enhances the adsorption ability of this surface. The growth of the structure conductance correlates with the magnitude of dipole moments of adsorbed polar molecules.

For Ti–TiO$_2$–n-Si structures, the growth of the adsorption sensitivity with increase of the applied voltage, which is associated with the growth in the number of conduction channels, is almost symmetric (Fig. 4,a). The growth of the conductance is favored by an increase of the diffusion length and a reduction of the recombination rate of injected electrons owing to the capture of charge carriers by traps. After the traps are filled, the electron transport in the oxide layer becomes almost dispersionless. The disordered TiO$_2$-300 specimens demonstrate a reduction of the adsorption sensitivity, which is associated with the fact that the percolation transport becomes complicated, and the charge carrier transport turns out restricted in nanoparticles with small dimensions [4].

For Ti–TiO$_2$–p-Si structures, the adsorption of polar molecules affects not only the current, but also the character of the dependence of the current on the applied voltage. If the injection currents are minimized (the positive polarity is applied to the Ti electrode), the adsorption sensitivity almost vanishes, which enables the sensitivity parameters to be controlled by varying the voltage polarity (Fig. 4,b).

4. Conclusions

The charge state of the internal surface in nanocrystalline TiO_2 substantially affects the process of charge carrier injection into the TiO_2 layer through a system of conduction channels. The formation of paths and the time of charge carrier transport depends on properties of the injecting contact, the nature and the filling degree of surface and bulk traps, and the local polarization of a nanocrystallite. The magnitude of compensating surface charge is determined by the type and the concentration of preceding and adsorbed surface centers. In Ti–TiO_2–p-Si structures, the variation of the ratio between the numbers of injected electrons and holes can induce the effect of negative conductance.

1. V.A. Skryshevsky, V.A. Vikulov, O.V. Tretyak, V.M. Zinchuk, F. Koch, and Th. Dittrich, Phys. Stat. Sol. A **197**, 534 (2003).

2. S.K. Hazra, S. Roy, and S. Basu, Mater. Sci. Eng. B **110**, 195 (2004).

3. G. Korotcenkov and B.K. Cho, Crit. Rev. Solid State Mater. Sci. **35**, 1 (2010).

4. S. Ben Amor, L. Guedri, G. Baud, M. Jacquet, and M. Ghedira, Mater. Chem. Phys. **77**, 903 (2002).

5. R. Komiya, J. Photochem. Photobio. A **164**, 123 (2004).

6. Th. Dittrich, V. Zinchuk, V. Skryshevskyy, I. Urban, and O. Hilt, J. Appl. Phys. **98**, 104501 (2005).

7. A. Ennaoui, B.R. Sankapal, V. Skryshevsky, and M.Ch. Lux-Steiner, Sol. Energy Mater. Sol. Cells **90**, 1533 (2006).

8. E.A. Konstantinova, V.Ya. Gayvoronskiy, V.Yu. Timoshenko, and P.K. Kashkarov, Semiconductors **44**, 1093 (2010).

9. P. Viswanathamurthi, N. Bhattarai, C.K. Kim, H.Y. Kim, and D.R. Lee, Inorg. Chem. Commun. **7**, 679 (2004).

10. O. Harizanov and A. Harizanova, Sol. Energy Mater. Sol. Cells **63**, 185 (2002).

11. Yingchun Zhu and Chuanxian Ding, J. Europ. Ceram. Soc. **20**, 127 (2000).

12. G. Kron, T. Egerter, J.H. Werner, and U. Rau, J. Phys. Chem. B **107**, 3556 (2003).

13. P.M. Kumar, S. Badrinarayanan, and M. Sastry, Thin Solid Films **358**, 122 (2000).

14. A. Zaban, A. Meier, and B.A. Gregg, J. Phys. Chem. B **101**, 7985 (1997).

15. V.A. Skryshevskyy, Th. Dittrich, and J. Rappich, Phys. Stat. Sol. A **201**, 157 (2004).

16. E.A. Lebedev and Th. Dittrich, Semiconductors **36**, 1268 (2002).

17. A.L. Fahrenbruch and R.H. Bube, *Fundamentals of Solar Cells: Photovoltaic Solar Energy Conversion* (Academic Press, New York, 1983).

18. A.Yu. Karlach, G.V. Kuznetsov, S.V. Litvinenko, Yu.S. Milovanov, and V.A. Skryshevsky, Semiconductors **44**, 1342 (2010).

19. V.B. Lazarev, V.G. Krasov, and I.S. Shaplygin, *Electric Conductivity of Oxide Systems and Film Structures* (Nauka, Moscow, 1979) (in Russian).

20. A.I. Manilov, A.M. Veremenko, I.I. Ivanov, and V.A. Skryshevsky, Physica E **41**, 36 (2008).

21. H. Wittmer, S. Holten, H. Kliem, and H. Breuer, Phys. Stat. Sol. A **181**, 461 (2000).

22. V. Kytin and Th. Dittrich, Phys. Stat. Sol. A **185**, 461 (2001).

ОСОБЛИВОСТІ ПРОТІКАННЯ СТРУМУ
В ГЕТЕРОСТРУКТУРАХ ОКСИД ТИТАНУ–КРЕМНІЙ

Ю.С. Мілованов, І.В. Гаврильченко, В.Я. Гайворонський, Г.В. Кузнецов, В.А. Скришевський

Р е з ю м е

Досліджено інжекційні механізми переносу носіїв заряду в гетероструктурах Ti–TiO_2–(n, p)Si. Розглянуто вплив структури пористого шару TiO_2 і типу кремнієвої підкладки на електричні характеристики структур. Перенос носіїв заряду відбувається за умов існування компенсуючого поляризаційного заряду на поверхні TiO_2 наночастинок. Встановлено кореляції між типом адсорбованих молекул і умовами проходження струму. У структурах Ti–TiO_2–pSi зміна співвідношення інжектованих електронів та дірок може приводити до ефекту негативної провідності.